Seismic Performance of Typical Tall Buildings in Singapore

Key Seng Goh, Kusnowidjaja Megawati & Tso-Chien Pan
School of Civil and Environmental Engineering, Nanyang Technological University, Singapore

SUMMARY:
The seismic performances of 15-storey and 30-storey generic models, which should represent typical tall buildings in Singapore, are examined. The natural period of the models are correlated with the natural periods of the actual buildings by conducting ambient vibration test. The modelling of the generic buildings is emphasized on the lightly reinforced beam-column joints and the bottom soft-storey effect. The beam-column joint model is evaluated by using the experimental data. The seismic responses of the structures located at a soft-soil site due to maximum credible earthquakes in Sumatra are examined. From the analysis, it is concluded that damage is less likely to occur in the generic models subjected to maximum credible Sumatran earthquakes ground motions.

Keywords: Singapore; Seismic Performance; Tall Building; Beam-column joint; Maximum Credible Earthquake

1. INTRODUCTION

Singapore is a modern city with a population of about 5 million living in an area of about 600 km^2 (Singapore Department of Statistics, 2011). Due to land shortage, more than 80% of the population in Singapore lives in high-rise residential buildings (Housing Development Board, 2009). Although Singapore is located in a low seismicity area, the country is exposed to long-distance earthquake originated from Sumatra. The long period ground motion may post certain threat to the high-rise buildings in Singapore, which may have natural periods close to the predominant period of the ground motion, especially the buildings located on soft-soil site. A good example of the potential risk posted by the long-distance earthquake is the Mexico earthquake which caused severe damages at an epicentral distance of about 350 km in 1985. Megawati and Pan (Megawati and Pan, 2002) has identified the maximum credible earthquakes in Sumatra to be a subduction earthquake (M_w=9.0) off the west coast of Sumatra and a fault earthquake (M_w=7.5) on the Great Sumatran Fault. The synthetic bedrock motions corresponding to the maximum credible Sumatra subduction earthquake and the fault earthquake have been simulated (Megawati and Pan, 2002).

The current building design code for structures in Singapore does not have any provision for seismic loading (BSI, 1997). It does, however, require that all buildings to be capable of resisting a notional ultimate lateral design load applied at each floor level simultaneously for structural robustness. These static lateral loads are equal to 1.5% of the characteristic dead weight of the structure. The beam-column joints of the structures are usually nonseismically detailed and their joint dimensions are unusual (Li et al., 2002). The nonseismically detailed beam-column joints may not be adequate to sustain earthquake-induced loads caused by large Sumatra earthquake. In this paper, the seismic performances of 15-storey and 30-storey generic models, which should represent typical tall buildings in Singapore, are examined. The beam-column joints are carefully modelled and they are compared with the experimental data. The responses of the generic models subjected to the maximum credible ground motions from Sumatra subduction earthquake and the fault earthquake are presented.

2. STRUCTURAL MODELLING

The structural modelling and analyses are run using the Open Source for Earthquake Engineering Simulation (OpenSEEs, 2002). Two generic models representing buildings of 15 and 30 stories are considered. The 15-story model represents typical building with rectangular plan (slab block) and the 30-story model is for buildings with square plan (point block) buildings (Figure 1). Both structural systems are commonly used for public housing in Singapore.

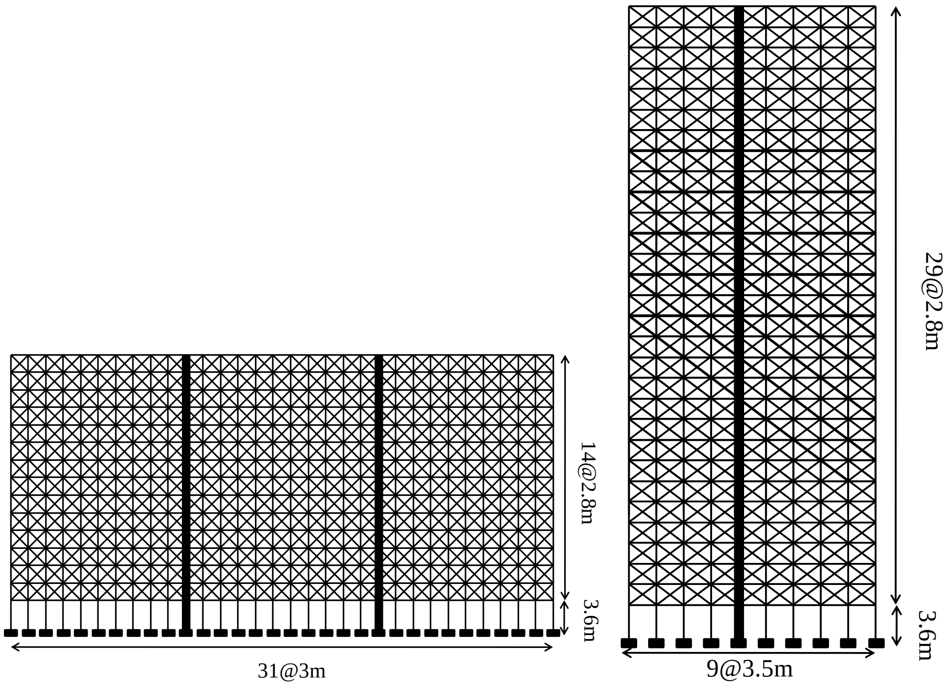

Figure 1. Graphical illustration of the 30-storey generic model

2.1 Generic Model Description

The model is reinforced concrete infilled frame building with shear wall. The height for 1st storey is 3.6 m, while the heights for 2nd storey and above are 2.8 m. For the 15-storey generic model, the bay width is 3 m, and there are 31 bays in total. For the 30-storey generic model, the bay width is 3.5m, and there are 9 bays in total. The masonry walls are modelled using equivalent diagonal struts model as proposed by Saneinejad and Hobbs (Saneinejad and Hobbs, 2995). The stress-strain relationship for masonry wall is based on the experimental data by Kaushik et al. (Kaushik et al., 2007). The 1st storey of the model is typically open space for public or social functions, thus diagonal struts are not modelled at the 1st storey. The masonry properties parameters are presented in Table 1.

The typical column and lift core wall sections are presented in Figure 2. The effect of slab is taken into account by using a beam-slab system. For the 15-storey model, the columns at the 1st to 3rd storey are modelled with column section A1 while the columns at the 4th to 15th storey are modelled as column section A2. For the 30-storey model, the columns at the 1st storey to 11th storey are modelled as column section A1 while columns at 12th to 30th are modelled as column section A2. The 11th and 22nd columns from left for the 15-storey model and 5th column from left for the 30-storey model are lift cores. The lift core wall, column and the beam-slab sections are modelled with fiber-based section elements, using force-based nonlinear beam-column elements with co-rotational geometric transformation and five Gauss-Lobatto integration points along the element length. The use of fiber-based with force-based formulation to model shear wall has been proven to be accurate and efficient (Martinelli and Filippou, 2009). The effective slab width of the beam-slab section is modelled to be equal to beam width plus three times beam depth, based on work by Pantazopoulou and Moehle (Pantazopoulou and Moehle, 1990). The modelling of beam-wide column joint will be discussed in the next session.

The concrete is modelled as uniaxial concrete material with tensile strength and linear tension softening. To quantify the confinement effects, the confined concrete model by Mander et al. is used (Mander et al., 1988). The steel is modelled as uniaxial steel material with isotropic strain hardening. The properties for unconfined concrete and steel materials are shown in Table 2. The masses are lumped at the joints. The column bases are fixed to the ground.

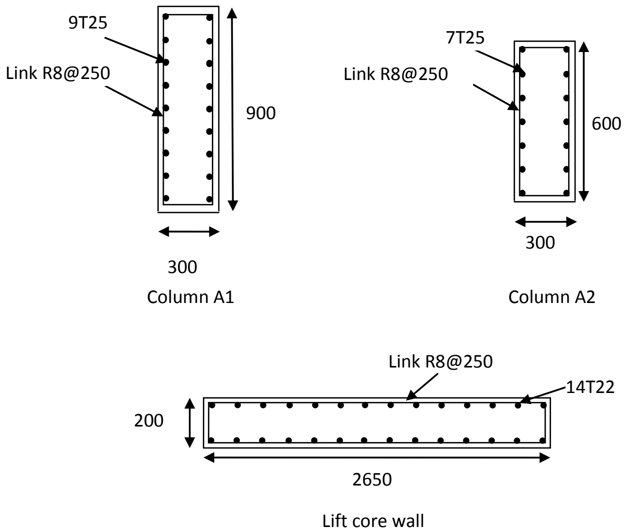

Figure 2. Summary of concrete frames elements (unit in mm)

Table 1. Summary of masonry wall properties parameters

Compressive strength, f_c (Mpa)	Strain at f_c, ε_{sc}	Crushing strength, f_{cu} (Mpa)	Strain at f_{cu}, ε_{su}
4.1	0.004	2.5	0.003

Table 2. Material properties for reinforced concrete frame elements

f_c	ε_{sc}	f_{cu}	ε_{su}	f_t	E_{ts}	F_y	E	b
30	0.002	6	0.003	2	500	460	200	0.01

f_c: Unconfined concrete compressive strength (MPa);
ε_{sc}: Unconfined concrete strain at f_c;
f_{cu}: Unconfined concrete crushing strength (MPa);
ε_{su}: Unconfined concrete strain at f_{cu};
f_t: Unconfined concrete tensile strength (MPa);
E_{ts}: Unconfined concrete tension softening slope (MPa);
F_y: Steel yield stress (MPa);
E: Steel modulus of Elasticity (GPa);
b: Steel hardening Ratio

2.2 Beam-column Joint Modelling

2.2.1 Experiment on beam-wide column joints

Four full-scale reinforced concrete interior beam-wide column joints with nonseismic detailing and limited seismic detailing were designed and tested to investigate the seismic behaviour of the joints (Li et al., 2002). The details of the experimental procedures and results can be found in the work by Li et al. (Li et al., 2002).

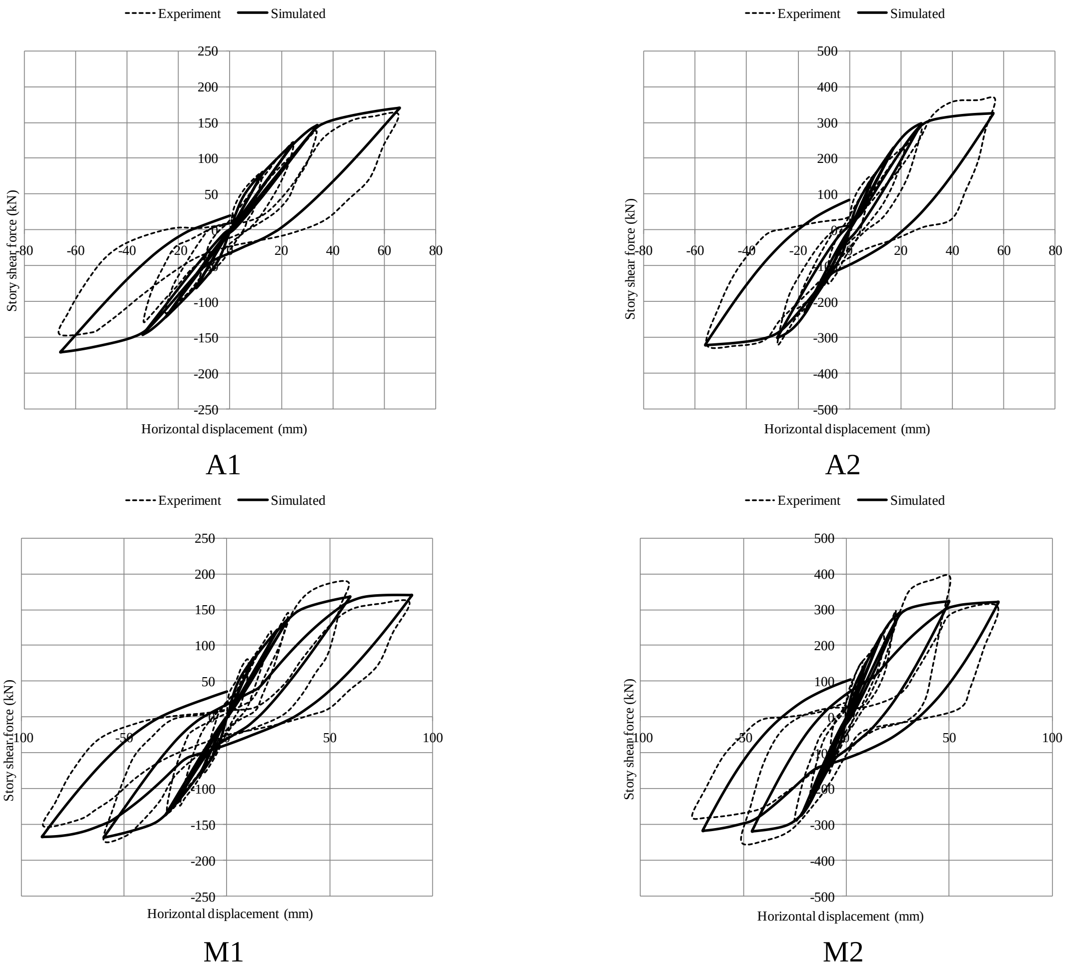

Figure 3. Comparison between the experimental and simulated results

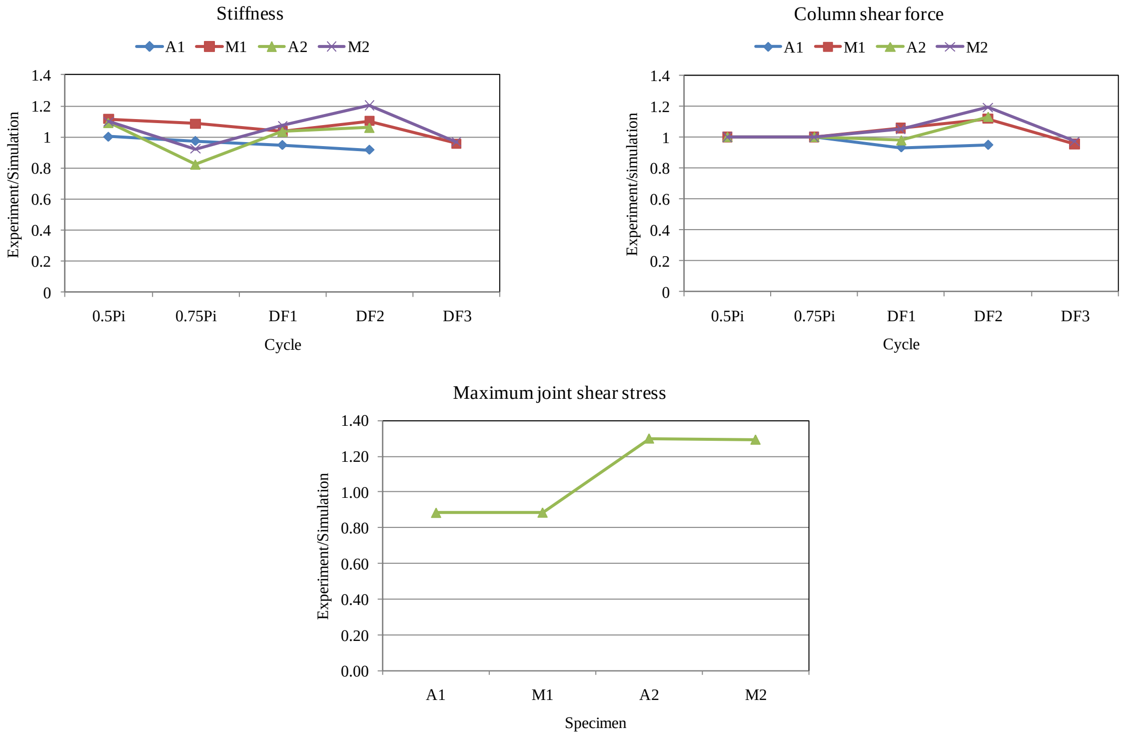

Figure 4. Summary of comparison between the experimental and simulated results

2.2.2 Simulation of Joint model

The two-dimensional joint model developed and implemented in OpenSEEs by Altoontash (Altoontash, 2004), is employed to model the beam-wide column joints. This model accounts for the finite joint size, and uses rotational springs and systems of constraints to model the shear panel behaviour and the bond-slip behaviour. The shear stress-strain response of the joint core is simulated by using the method proposed by Mitra and Lowes (Mitra and Lowes, 2007). The joint shear in the core region is assumed to be transferred through a confined concrete strut. Bilinear idealization has been adopted to model the stress strain behaviour of the joint core region. The hysteretic behaviour of the joint shear panel is modelled based on recommendations by Altoontash (Altoontash, 2004), who proposed that the hysteretic behaviour be pinched and have a pinch-point at 25% of the maximum historic stress and 25% of the maximum historic strain. The bond-slip at the end of the beam and column connections are not modelled as they are found to be insignificant in affecting the overall behaviour of the joint (Li et al., 2002).

2.2.3 Comparison

The comparisons between the experimental and simulated results are shown in figure 3. From figure 3, it can be seen that the simulation by the joint model can accurately predict the behaviour of the joint. Pinching can be found in the simulated results, and this is very similar to the behaviour of the joints from the experiment. Figure 4 summarizes the comparison between the experimental and simulated results in terms of stiffness, column shear force and maximum joint shear stress. It can be concluded that the joint model prediction is reasonably well-matched with the experimental results. The differences between the experimental and simulated results are kept within 30%. Thus it is concluded that the joint model can be used to predict the behaviour of the nonseismically detailed beam-wide column joints.

2.3 Validation of Generic Model

In order to correlate the natural periods of the simulated generic models with the natural periods of actual buildings, ambient vibration tests have been conducted on the actual buildings in Singapore. Two 15-storey and two 30-storey buildings are selected for this purpose. Fast Fourier Transform is used to estimate the natural periods of the buildings by peak-picking method. The natural periods of the two measured 15-storey slab blocks are found to be 0.65 s and 0.72 s, while for the 30-storey point blocks, the natural periods are found to be 1.32 s and 1.37 s. The eigenvalue analysis shows that the first natural period of the 15-storey generic model is 0.65 s, while the first natural period of the 30-storey model is 1.32 s. By comparing the natural periods of the measured buildings with the natural periods of the 15 and 30-storey generic models, it is found that the values of natural periods of the generic models fall within the range of the natural periods of the two measured buildings. Thus it is reasonable to use the generic models to represent the typical 15-storey slab blocks and 30-storey point blocks in Singapore.

3 MAXIMUM CREDIBLE EARTHQUAKES

It has been identified that the maximum credible ground motions in Singapore are likely to be caused by two large earthquakes with different source mechanism (Megawati and Pan, 2002). One is the fault earthquake (Sumani segment) with an epicentral distance of around 425 km and a moment magnitude of 7.5. The other is a Sumatra subduction earthquake with an epicentral distance of 700 km and a moment magnitude of 9.0.

Figure 5 shows the $\mu+\sigma$ acceleration response spectra (5% damping ratio) in Singapore resulting from the maximum credible fault earthquake (M_w=7.5, R= 425 km) and the maximum credible subduction earthquake (M_w=9.0, R= 700 km) respectively. The acceleration response spectral for Sumatran fault is estimated using the attenuation relationship derived by Megawati (personal communication with

Kusnowidjaja Megawati), while the acceleration response spectral for Sumatran subduction is estimated using attenuation relationship derived by Megawati and Pan (Megawati and Pan, 2010).

For assessment of seismic performance of high-rise buildings in Singapore due to the maximum credible Sumatran fault and subduction earthquake, 6 sets of recorded Sumatran fault ground motions and 10 sets of recorded Sumatran subduction ground motions in Singapore are considered. The recorded Sumatran fault ground motions are scaled to match the target spectrum due to maximum credible fault earthquake, while the recorded Sumatran subduction ground motions are scaled to match the target spectrum due to maximum credible Sumatran subduction earthquake. The comparison between the target and matched spectrum are shown in Figure 5.

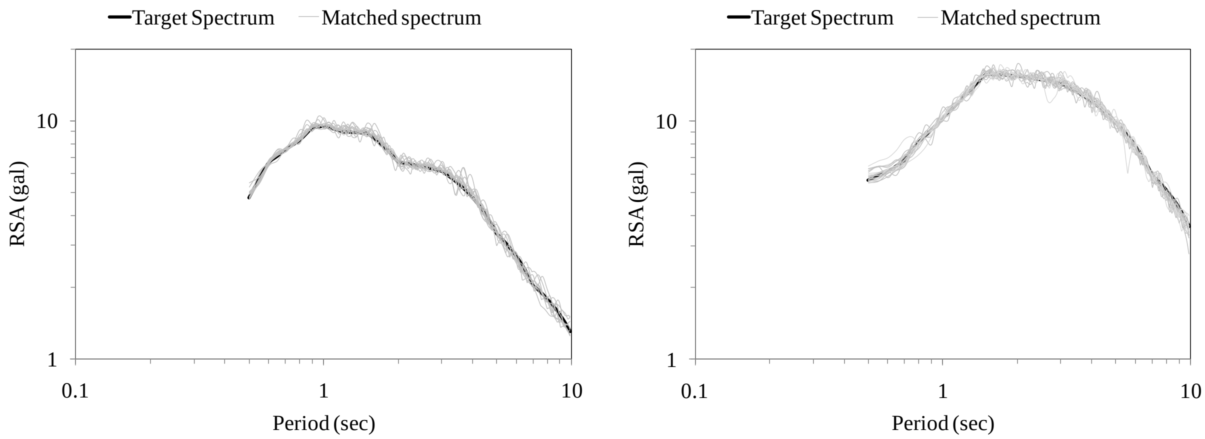

(a) (b)

Figure 5. 5%-damped elastic spectral response from records matched to the 5%-damped target spectral acceleration for maximum credible (a) Sumatran Fault earthquakes; (b) Sumatran Subduction earthquakes.

3.1 Effects of Soft-Soil Amplification in Singapore

It should be noted that the ground motions generated shown in Figure 5 are for rock site. The central and southeastern parts of Singapore Island are largely overlain by Quaternary marine clay deposits, and a significant portion of the southern coastal area is reclaimed land (Pitts, 1984). This soft soil deposits can significantly amplify the weak bedrock motion, as confirmed by recent Sumatran earthquakes where tremors were largely felt by residents of high-rise buildings in these areas and not in other areas with better ground conditions. Since seismic-resistant design is not required in Singapore, buildings on soft-soil and rock sites are designed against the same lateral loads, resulting in buildings with the same seismic capacity. The seismic risk to structures on soft soil sites is, therefore, higher than those on firm-soil or rock sites, simply because the seismic hazard level is higher at the soft-soil sites.

Table 3 shows the soil profile at a soft soil site, which are overlain by marine clay deposit (the Kallang formation), in the southern part of Singapore. The Shear-wave velocity profiles were obtained by crosshole PS logging. These are typical soft-soil profiles in Singapore, having average shear-wave velocity values of the upper 30 m ($V_{S,30}$) of 130 m/s. According to the 2000 edition of the International Building Code (IBC, 2000), both sites are classified as soft soil (Site Class E) based on the value of $V_{S,30}$.

The site response analysis is carried out using the equivalent linear model of the horizontally-layered soil deposit, as implemented in the widely-used computer program called SHAKE91 (Schnabel et al., 1972; Idriss and Sun, 1992). In the equivalent linear method, nonlinear behavior of soil is accounted for by the use of strain-dependent stiffness and damping parameters. The stiffness of the soil is characterized by the maximum shear modulus $G_{\max}$ and a modulus reduction curve, showing how the shear modulus G decreases from $G_{\max}$ at larger strain. Damping behavior is characterized by the damping ratio, which increases with increasing strain amplitude. The present study uses the $G/G_{\max}$

and damping ratio curves developed by Seed and Idriss (Seed and Idriss, 1970) for cohesionless soils, and the curves proposed by Vucetic and Dobry (Vucetic and Dobry, 1991) for cohesive soils. More details about the soft-soil site amplification can be found in the work by Megawati and Pan (Megawati and Pan, 2009). Figure 6 shows the response spectral acceleration at the soft-soil site due to the maximum credible fault and subduction earthquakes and the corresponding spectral amplifications.

Table 3. Soil profiles of the soft-soil site, which is overlain by marine clay deposit.

Formation	D (m)	V_S (m/s)	ρ (t/m^3)	PI
Fill (sandy soil)	6.5	120	1.67	Low
Upper marine clay	13	120	1.61	30
Clay	2	190	1.94	30
Lower marine clay	9	145	1.69	30
Organic clay	4	225	1.62	30
Residual soil	5	235	2.07	15
Slightly weathered silty sand	5.9	225	2.07	15
Slightly weathered silt	4.6	440	2.11	Low

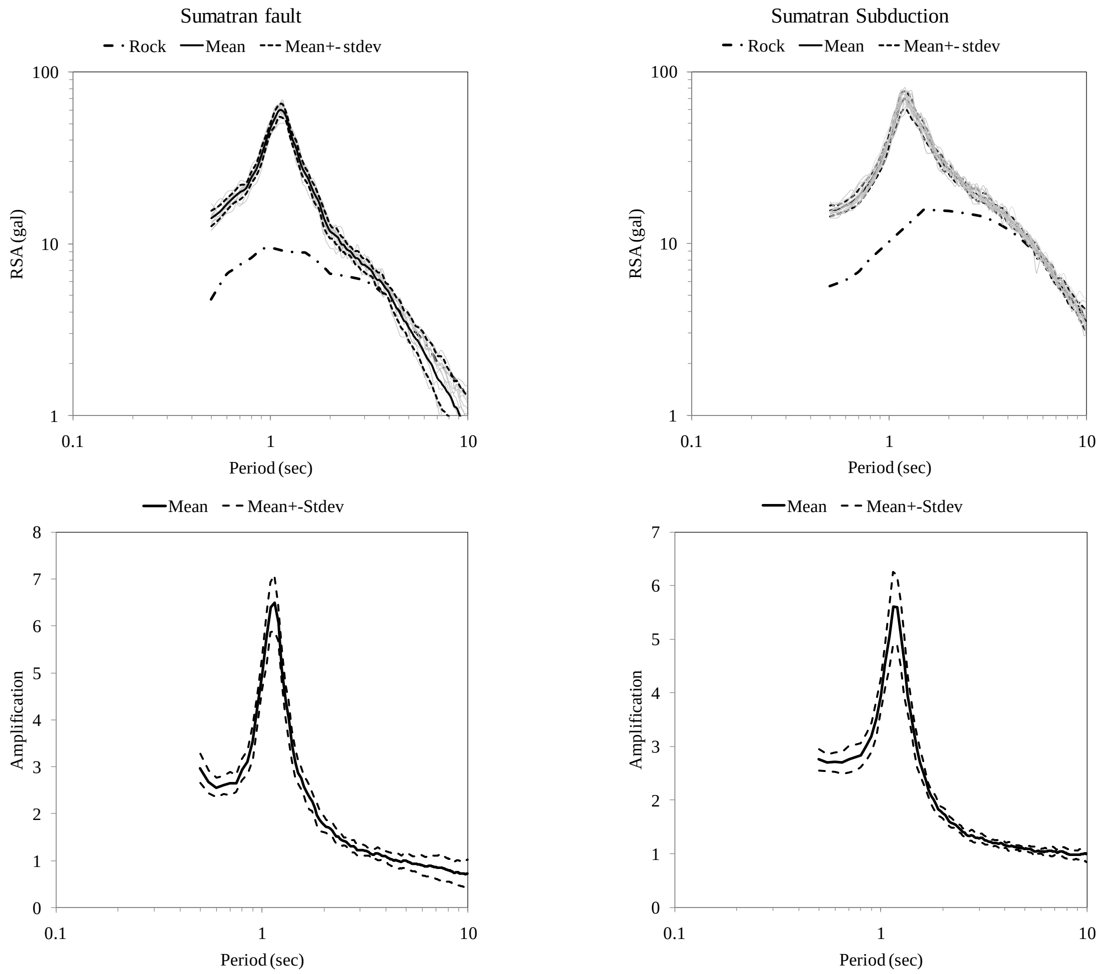

Figure 6. Spectral acceleration at soft-soil site and the corresponding amplification factors between the surface and bedrock

4 NONLINEAR DYNAMIC ANALYSIS

The nonlinear dynamic analyses are conducted using OpenSEEs (OpenSEEs, 2002). The damping ratio is assumed to be 5%. Newmark integrator is used in the analysis. Figure shows the maximum inter-storey of the 15-storey and 30-storey generic models subjected to maximum credible ground motions at both rock and soft-soil sites. At rock site, the 15-storey generic model has slightly larger response than the 30-storey generic model. In contrast, at soft-soil site, the 30-storey generic model has larger response than the 15-storey generic model. In general, at soft-soil sites, the two generic models have larger response when subjected to maximum credible subduction earthquakes than maximum credible fault earthquakes.

Figure 8 shows the maximum normalized joint shear stress induced in the 15-storey and 30-storey generic models subjected to maximum credible earthquakes ground motions. For both structures, the joint shear stresses induced are below the shear strength of the joints. This implies that the joint shear failure is less likely to occur in the joints when the generic models are subjected to maximum credible ground motions.

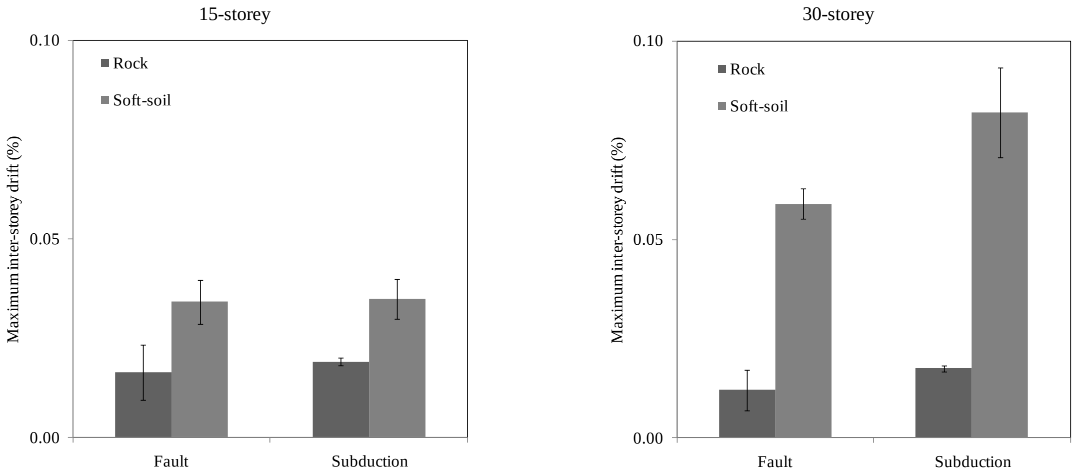

Figure 7. Maximum inter-storey drift ratio of the 15-storey and 30-storey generic models subjected to maximum credible ground motion at rock and soft-soil site. Error bars represent standard deviations of the results.

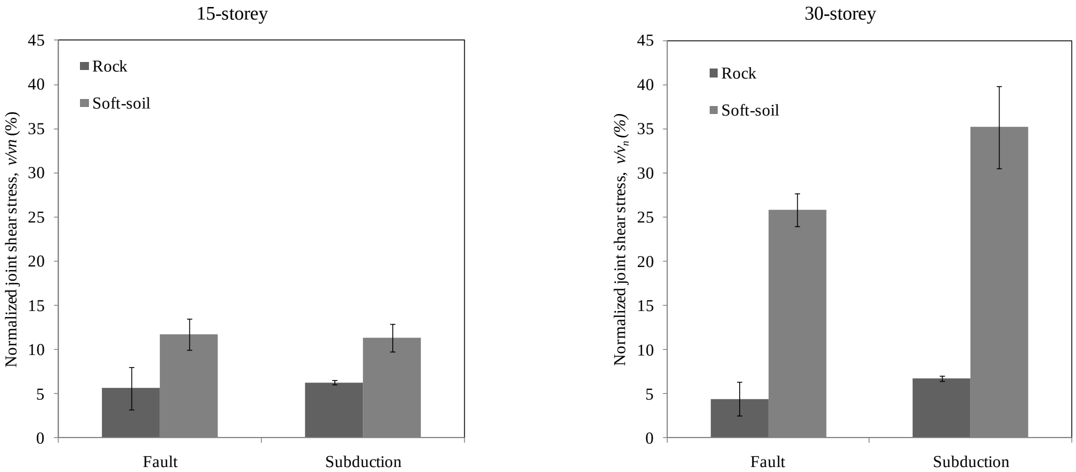

Figure 8. Maximum joint shear stress induced in the 15-storey and 30-storey generic models subjected to maximum credible ground motion at rock and soft-soil site. Error bars represent standard deviations of the results.

6 CONCLUSIONS

In this paper, a 15-storey and 30-storey generic models are constructed. Special attention is given to the modelling of beam-wide column joints. Comparison has been done between the experimental and simulation results of the beam-wide column joints and they are found to be satisfactory. The seismic response of the generic model subjected to the maximum credible Sumatra fault and subduction earthquake at both rock and soft-soil sites are examined by conducting nonlinear dynamic analysis. From the analysis, it is concluded that the generic models are less likely to be damaged during the maximum credible earthquakes.

REFERENCES

Altoontash, A. (2004). Simulation and damage models for performance assessment of reinforced concrete beam-column joints. PhD Dissertation, California, Stanford University, USA.

British Standard Institution (1985). Structural Use of Concrete, Part 1. Code of Practie for Design and Construction.

Housing Development Board (2009). HDB Annual Report 2008/2009. Singapore.

Idriss, I. M. and J. I. Sun (1992). User's manual for SHAKE91, Center for Geotechnical Modeling, Department of Civil Engineering, University of California, Davis.

International Code Council (2000). International Building Code, year 2000 edition.

Kaushik, H. B., D. C. Rai and S. K. Jain (2007). Stress-strain characteristics of clay brick masonry under uniaxial compression. Journal of Materials in Civil Engineering **19:9**, 728-739.

Li, B., Y. Wu and T. C. Pan (2002). Seismic behavior of nonseismically detailed interior beam-wide column joints - Part I: Experimental results and observed behavior. ACI Structural Journal **99:6**, 791-802.

Mander, J. B., M. J. N. Priestley and R. Park (1988). Theoretical Stress-Strain Model For Confined Concrete. Journal of structural engineering New York, N.Y. **114:8,** 1804-1826.

Martinelli, P. and F. C. Filippou (2009). Simulation of the shaking table test of a seven-story shear wall building. Earthquake Engineering and Structural Dynamics **38:5**, 587-607.

Megawati, K. and T. C. Pan (2002). Prediction of the maximum credible ground motion in Singapore due to a great Sumatran subduction earthquake: The worst-case scenario. Earthquake Engineering and Structural Dynamics **31:8,** 1501-1523.

Megawati, K. and T. C. Pan (2009). Regional Seismic Hazard Posed by the Mentawai Segment of the Sumatran Megathrust. Bulletin of the Seismological Society of America **99:2A**, 566-584.

Megawati, K. and T. C. Pan (2010). Ground-motion attenuation relationship for the Sumatran megathrust earthquakes. Earthquake Engineering and Structural Dynamics **39:8,** 827-845.

Mitra, N. and L. N. Lowes (2007). Evaluation, calibration, and verification of a reinforced concrete beam-column joint model. Journal of Structural Engineering **133:1**, 105-120.

OpenSEEs (2002). Open System for Earthquake Engineering Simulations. Berkerly, CA.

Pantazopoulou, S. J. and J. P. Moehle (1990). Identification of effect of slabs on flexural behavior of beams. Journal of Engineering Mechanics **116:1,** 91-106.

Pitts, J. (1984). A review of geology and engineering geology in Singapore. Quarterly Journal of Engineering Geology **17:2**, 93-101.

Saneinejad, A. and B. Hobbs (1995). Inelastic design of infilled frames. Journal of structural engineering New York, N.Y. **121:4**, 634-649.

Schnabel, P. B., J. Lysmer and H. B. Seed (1972). SHAKE: A computer program for earthquake response analysis for horizontally layered sites, Earthquake Engineering Research Center, University of California, Berkeley.

Seed, H. B. and I. M. Idriss (1970). Soil moduli and damping factors for dynamic response analysis, Earthquake Engineering Research Center, University of California, Berkeley.

Singapore Department of Statistics. (2011). Monthly Digest of Statistics Singapore. Singapore.

Vucetic, M. and R. Dobry (1991). Effect of soil plasticity on cyclic response. Journal of geotechnical engineering **117:1**, 89-107